COMPUTATIONAL MODELING IN BIO-HYDRODYNAMICS: TRENDS, CHALLENGES AND RECENT ADVANCES

Rajat Mittal
Department of Mechanical and Aerospace Engineering
The George Washington University
mittal@gwu.edu

Abstract—**Computational modeling is assuming increased significance in the area of bio-hydrodynamics. This trend has been enabled primarily by the widespread availability of powerful computers as well the induction of novel numerical and modeling approaches. However, despite these recent advances, computational modeling of flows in complex bio-hydrodynamic configurations remains a challenging proposition. This is due to a multitude of factors including the need to handle a wide range of flow conditions (laminar, transitional and turbulent), the ubiquity of two-way coupled interaction between the fluid and moving/deformable structures and finally, the requirement of accurately resolving unsteady flow features. Recently, as part of an ONR sponsored review, the objective of which was to distill the science related to biology-based hydrodynamics for maneuvering and propulsion, an extensive survey of computational bio-hydrodynamics was undertaken. The key findings of this survey are reported in this paper**

Index Terms—**Bio-hydrodynamics, computational modeling, numerical simulation, computational fluid dynamics**

I. Introduction

EXPERIMENTAL investigations in bio-hydrodynamics are limited by their inability to provide full-field, spatially and temporally resolved, velocity and pressure measurements. Some of these limitations are intrinsic to the methods being used whereas others are associated with the specific conditions associated with bio-hydrodynamics. Chief among these are the conditions imposed by the need to work with live animals since it is often difficult to control/predict the motion and location of these animals under test conditions. Methods for controlling the subject that are overly invasive (such as tethering or excessive confinement), run the risk of modifying the natural motion/gait of the subject. In addition to the traditional approach of painstakingly conditioning the subjects to respond somewhat predictably in test conditions, recently, some novel control methods based on visual stimuli have been employed (www.dickinson.caltech.edu/research_visualflightcontrol.html) which might hold promise for future studies. However, even if some amount of repeatability and control can be instilled in these tests through some minimally invasive means, it is usually difficult to instrument the test subjects with sensors to the extent needed without disrupting the natural behavior of the subject. For instance, no method currently exists for extracting the surface pressure and shear stress distribution on a structure as delicate as the flapping pectoral fin of a boxfish. Such measurements are of critical importance since they allow for direct measurement of the hydrodynamical performance of the locomotor under consideration and would also provide good insight into the flow physics. The final hurdle faced by experiments is the need to make measurements in the vicinity of bodies/boundaries that are undergoing large motions since this causes problems for invasive (hot wire probes etc.) as well as non-invasive (LDV, PIV etc) measurement methods. Some of the above limitations have motivated the development of articulated mechanical models of these animals [1], which can be controlled and instrumented in a manner adequate for detailed engineering analysis.

Another approach that holds the potential for overcoming most of the above limitations is computational modeling. In order to examine the challenge posed by bio-hydrodynamics to computational modeling and simulation, consider the swimming of the bluegill sunfish (*Lepomis macrochirus*) (fig. 1) that has been the subject of a detailed study by Drucker and Lauder [2]. Depending on the gait, the pectoral, median as well as tail fins can all be involved in propulsion and maneuvering. For typical specimens, the Reynolds number based on the fish body length (L~20cm) and velocity ($0.5\ Ls^{-1}$) is about 20,000. At this Reynolds number, the attached flow over the body is most likely laminar but is expected to transition rapidly to turbulence in regions of flow separation which might occur downstream of appendages. The fins of this fish are also highly flexible, have complex planforms and undergo complicated motions. The flow over the fins can be characterized in terms of a Stokes frequency parameter ($S = \omega A l / \nu$ where ω, A and l are the fin angular frequency, amplitude and length respectively). Typical fin beat frequency of about 3 Hz and fin amplitude and size of about 2cm and 5cm respectively gives $S \approx 18{,}000$ which is again in the range where laminar attached flow would quickly transition to turbulence post separation. It is worthwhile to point out that flow separation and transition to turbulence from a fin can not only have a large impact on the hydrodynamic loading of that fin, it can also alter drastically, the flow conditions experienced by any downstream fins/appendages.

Thus, assuming that the above conditions are prototypical of bio-hydrodynamic flow configurations, especially in the context of low-speed maneuvering, the key factors to be considered in computational modeling of these configurations

Rajat Mittal is with The George Washington University, Washington DC 22052 USA (phone: 202-994-9394, fax: 202-994-0238, e-mail: mittal@gwu.edu).

are:

a. Wide Range of Flow Conditions: Typical Reynolds numbers for swimming fishes/cetaceans can vary from $O(10^2)$ to $O(10^7)$. The flow can be laminar, transitional or turbulent or a combination of all three. In addition, the surrounding flow environment can be steady or unsteady.

b. Moving Boundaries: Bio-hydrodynamic flows of interest are often associated with moving boundaries, may they be flapping fins or undulating bodies.

c. Two-Way Fluid-Structure Coupling: In many cases the control surfaces (fins, appendages etc) are highly flexible and can undergo large deformations as a result of the hydrodynamic loading. This deformation can in turn have a significant effect on the flow, which can then alter the loading itself. In some situations the internal structural stress distribution may be of as much interest as the external hydrodynamics.

d. Unsteady Flow Mechanisms: The presence of moving and flexible control surfaces and/or the unsteady flow environment leads to configurations where dominance of unsteady flow mechanisms (added mass effects, dynamic stall, vortex shedding, vortex pairing, vortex-body and vortex-fin interactions) is a rule rather than an exception.

Until about a decade ago, it was not feasible to simulate such flows with all of their attendant complexities. However, the rapid increase in computing power and the availability of sophisticated simulation software has now brought these simulations within the realm of possibility. In the following sections, we summarize the state-of-the-art in computational modeling and simulation as it pertains to bio-hydrodynamics. This includes a critical evaluation of computational approaches used to date and a survey of other approaches that hold promise in this area. Furthermore, we examine the information that has been gleaned from these simulations *viz-a-viz* its impact on our understanding of bio-hydrodynamic phenomena.

II. Overview of Computational Approaches: Capabilities and Limitations

A. Flow Modeling

Both inviscid and viscous flow models have been employed in past studies in bio-hydrodynamics. Inviscid flow simulations are relatively inexpensive but carry the usual weaknesses inherent in this approach. In addition, their application to bio-hydrodynamic flows can be further limited by the fact that these flows are often dominated by separated shear layers and associated vortex structures which are a direct consequence of viscous effects. However, examination of results from inviscid computations serves the purpose of clearly delineating the flow regimes where viscous flow mechanisms are dominant. Furthermore, these computations are quite inexpensive and allow for rapid estimation of hydrodynamics forces and other gross flow features over a large parameter space. Examples of application of these methods to bio-hydrodynamics flows can be found in Refs. 3-11. However, inviscid models have a limited range of validity and given that viscous flow computations of these flows are well within the reach of present day computers, we focus primarily on viscous flow models.

The inclusion of viscous effects immediately raises the possibility of transition and turbulence, both of which have then to be accounted for in the simulations. A number of different options are available for modeling flow turbulence in numerical simulations and these are discussed here in the context on bio-hydrodynamic flows.

A.1 Reynolds-Averaged Navier Stokes (RANS) Modeling

In this approach the spatial and temporal resolution is such that almost none of the turbulence scales can be resolved and the effect of these scales has to be accounted for through turbulence models. A wide variety of models are available [12] although two models that have found widespread use in the bio-hydrodynamic community are the Baldwin-Lomax [13] and the Spalart-Allmaras [14] models. For flows that are steady in the mean, RANS simulations typically compute only the mean flow quantities. However, for flows with a large-scale, externally imposed unsteadiness, such as that encountered in bio-hydrodynamics, RANS is carried out with time-accurate schemes where an attempt is made to compute directly and resolve the large scales associated with this unsteadiness.

RANS has found widespread use in the engineering community as a relatively inexpensive tool for flow analysis. Its obvious advantage over inviscid models is that it can account for viscous effects. At a basic level, this eliminates the D'Alembert's Paradox which accounts for erroneous prediction of inviscid models for flapping foils at small amplitudes, In addition, viscous models no longer require imposition of the trailing-edge flow tangency condition and therefore allow for flow separation at any location on the foil/body. This is of critical importance for flapping foils, since leading-edge stall is considered a key mechanism in these flows. As will be discussed later, the big advantage that RANS has over other viscous modeling approaches (such DNS and LES) is that it is relatively inexpensive even for the complex configurations that are usually encountered in bio-hydrodynamics.

The main limitations of RANS approach are the following: RANS provides only limited information about the flow. Even for time-accurate simulations of unsteady flows such as those encountered in bio-hydrodynamics, the RANS simulations are designed to include only the largest flow structures (those that scale with the dominant flow length scale) in the flow and the smaller scales are not included. The extent to which the absence of the smaller flow structures affects the prediction of the larger vortex structures is quite problem dependent and usually cannot be judged *a-priori*.

The second issue with RANS is with regards to its ability to

predict separation and separated flows. Since most turbulence models used in conjunction with RANS assume that the flow at the wall follows the behavior of a canonical attached boundary layer, prediction of flow separation has always been accepted as a weakness of this method. This is especially the case where the separation occurs over gently curving surfaces due to an adverse pressure gradient. In cases where the separation is "massive" (e.g. leading edge stall over a pitching airfoil) this might not be a significant issue. However, even if separation is predicted correctly, conventional RANS approaches do not usually provide a reliable prediction of the flow in the separated region. The flow in these regions is highly non-homogeneous and anisotropic, and conventional turbulence models do not perform well under these conditions. Consequently, computed results can exhibit significant model dependence.

The final limitation of RANS models is their applicability to relatively low-Reynolds numbers flows. Conventional turbulence models are designed for classical high Reynolds number turbulence flows. Their application to flows at lower Reynolds numbers where the flow is transitional is more problematic. Typical Reynolds numbers in low-speed maneuvering situations are $O(10^4)$ which falls very much in the transitional range. For these flows, turbulence models specially designed for low-Reynolds number flows [12] might be more appropriate. However, even with these models, issues such as *ad-hoc* specification of transition could diminish the predictive capability of RANS for such flows.

Examples of the application of RANS to bio-hydrodynamic flows can be found in the work of Jones & co-workers, Ramamurti & co-workers, Tuncer and co-workers and Isogai et al. Some of the key results from these simulations will be discussed in later sections. Here we make some general comments about the previous RANS computations. Except for those by Ramamurti et al [8] who use a finite-element method, all of the other RANS simulations mentioned above have employed structured finite difference/volume methods. Usually little detail is provided regarding the turbulence model, but a review of these papers indicates that most assume that the flow is turbulent everywhere and Baldwin-Lomax algebraic turbulence model seems to be the method of choice [15].

A.2 Direct Numerical Simulation (DNS)

On the other end of the spectrum of flow modeling approaches from RANS is DNS, where the grid and temporal resolution is such as to resolve all the turbulence scales down to the dissipation range (see fig. 2). Thus, in DNS there is no need for including a turbulence model and this type of modeling procedure should be expected to give results with incomparable accuracy. Furthermore, these simulations provide temporally and spatially accurate information about all the scales in the flow including turbulence statistics, frequency spectra as well as vortex dynamics, thereby allowing a comprehensive analysis of flow. However, this detailed information comes at a very high cost and it has been estimated that the grid requirement of a DNS scales as $Re^{9/4}$. [16]. Consequently, DNS is limited to relatively low Reynolds numbers and it is difficult to find in literature, adequately validated direct numerical simulations of relatively complex flows for Reynolds numbers greater than about a few thousand [17,18]. This range of Reynolds number would seem to allow for investigation of low-speed maneuvering bio-hydrodynamics except that DNS is limited to relatively simple flows such as bluff-body wakes [17-19]. Even for these flows, CPU costs can be enormous. For instance, DNS of flow past a sphere at Re_d=1000 required about 1000 CPU hrs on a 195 MHz SGI Origin 2000 computer [18]. One of the first applications of DNS to flows with a relatively complex moving boundary was by Newman & Karniadakis [20] who simulated flow past a flexible cable using a spectral-element method. However, DNS has yet to be applied to flows as complex as a flexible, flapping pectoral fin. All of the necessary ingredients for performing such simulations (numerical methods and software) already exist and with the widespread availability of high-performance, large, parallel computers it is expected that such simulations will become feasible in the next few years.

A.3 Large-Eddy Simulation (LES)

This approach lies between the RANS and DNS approaches. In LES, a time-accurate simulation is carried out with resolution sufficient to resolve all of the energy containing scales down to the inertial subrange (see figure 2). Only the scales not resolvable on the mesh are modeled through a subgrid-scale (SGS) turbulence model. Furthermore, since all the energy containing scales are resolved directly, these simulations provide data for a wide range of dynamically significant scales in the flow and are therefore capable of predicting higher order statistics as well as frequency spectra.

Since, the dissipation scales are not resolved, the resolution requirements for LES are lower than a DNS for the same flow. Simplified estimates indicate that the grid requirement for LES scales as Re^2 [21], which is a slower increase than that for DNS. From a practical point of view, extensive experience with a variety of flows indicates that LES can extend the Reynolds number range by about one order of magnitude over a DNS carried out on the same mesh. Thus LES of flows in relatively complex geometries with Reynolds numbers up to about 10,000 have been carried out where extensive validation against experimental data have confirmed the accuracy of the computed results [22]. One of the largest large-eddy simulations being carried out currently is that of the rotor-tip clearance flow [23] at a Reynolds number of 400,000 These simulations are being carried out in close coordination with a companion experimental study [24] and the objective is to demonstrate through extensive validation, that LES can accurately compute the details of this flow. Some results from these simulations are included here in order to demonstrate the type of data that can be obtained from LES. Figure 3a shows the flow configuration. Figures 3(b) and 4 shows some

representative comparisons between experiments and LES. The grid employed for these simulations has over 25 million mesh points and one simulation requires on the order of 10^5 single node CPU hrs on a SGI-Origin 3000. The simulations are made feasible through a DoD HPCC Challenge Grant, which provides access to and priority on some of the largest DoD computers.

It should be pointed out that in LES, since only the subgrid scales are modeled, there is less sensitivity to the model parameters. Furthermore, the introduction of the dynamic SGS model [25] has removed most of the *ad-hoc* parameter adjustments that are prevalent in RANS computations. In the dynamic modeling procedure, the eddy viscosity is computed during the computation by estimating the energy being transferred from the resolved to the SGS modes. Furthermore, the dynamic model automatically detects laminar regions and turns off. It is also capable of predicting transition and automatically produces the correct wall behavior. Thus, LES with dynamic model is quite well suited for prediction of complex flows.

Based on our previous experience we estimate that LES of a flapping pectoral fin operating at a Reynolds number of about 18,000 would require on the order of 20,000 single node CPU hours on a current generation computer. Here we have assumed that the presence of a moving boundary, will approximately double the cost of the computation. Therefore on a 32-node parallel computer, one simulation could be turned around in about 26 days. Therefore, such computations are very much within the realm of possibility. Given that the LES methodology provides data sufficient for examining the flow mechanisms underlying low-speed maneuvering bio-hydrodynamics, it should emerge as the methodology of choice in the coming years. Note that a DNS of the same flow would require a two or three fold increase in the CPU requirement.

A.4 Detached-Eddy Simulation (DES)

As discussed above, LES is clearly a useful tool for detailed analysis of the physics of bio-hydrodynamic flows. However, given the significant computational resources required, LES would not be well suited for covering a large parameters space. It would also not be appropriate for instance, for rapid engineering analysis of bio-robotic pectoral fins. For these tasks one would typically turn to the RANS approach. However, as discussed above, the predictive capability of RANS can be seriously compromised in separated flows such as those found for flapping foils. The RANS method is designed to model the entire spectrum of turbulent motions. While this might be adequate for simple attached flows, RANS turbulence models are unable to accurately predict phenomena occurring in flows that exhibit large separation. Unsteady massively separated flows are characterized by geometry dependent eddies, the affect of which cannot be represented well in RANS turbulence models. In order to overcome some of these deficiencies, a new approach termed Detached-Eddy Simulation (DES) has been proposed which combines element of RANS and LES. This approach can be considered a modification of the RANS approach where the geometry dependent, unsteady turbulent motions in the separated flow region are resolved. Separated flows computed using this approach, have shown marked improvement in accuracy over corresponding RANS computations. Figure 5 and 6 show comparisons between RANS, DES and experiments for flow past a forebody at large angle-of-attack computed by Squires et al. [26]. The DES clearly captures more of the unsteady nature of the separated flow and yields a very good comparison with the experiment for the pressure distribution. Many other similar examples indicate the advantage of this approach over RANS [26]. It is also important to note that this approach is formulated in a way such that it reverts back to the conventional RANS approach for attached flows. Furthermore, the computational expense of this approach is higher than that of a corresponding RANS but significantly less than a corresponding LES. Based on the above discussion, it would seem that DES would be preferable over RANS for rapid analysis of bio-hydrodynamic flow configuration.

B. Numerical Methodology

The type of grid employed quite often distinguishes one numerical simulation methodology from another. The following describes the various types of grids that are available along with comments on the suitability of each type of grid for bio-hydrodynamic flows.

B.1 Body conformal methods

The conventional approach to simulate flows with complex boundaries is to generate a body-conformal grid, i.e. a grid that conforms to the shape of the boundaries. Within this approach two different types of grids are employed; the structured grid and the unstructured grid.

Figure 7a shows an example of a structured curvilinear grid generated around an airfoil section. The key advantage of structured grid methods is that discretization of conservation laws on these grid lead to systems of equations that are amenable to powerful Line/Block-SOR iterative technique. These methods work well for relatively simple geometries. As the geometry gets more complex, single-block grids might not suffice and one has then to turn to multi-block meshes. However, in configurations where complex moving boundaries are present such as those common in bio-hydrodynamics, even conventional multi-block structured grid methods would be difficult to work with. For such flows, overset structured grids [27] offer the greatest potential. An example of an overset grid generated for a multi-component airfoil is shown in figure 7(b). In this configuration, the movable trailing-edge flap is surrounded by a body conformal curvilinear structured grid (yellow grid) which overlays the grid for the airfoil. As the flap moves, only the overset (yellow) grid moves whereas the underlying grid is unaffected.

Unstructured grid method methods are better suited than structured grid method for simulation of bio-hydrodynamic flows due to their ability to handle complex geometries. Figure 8 shows an unstructured grid generated around an airfoil. Unstructured grid methods can be used in conjunction with finite volume, finite element or spectra element type discretization methods. For example, Ramamurti and Sandberg [28] have used conventional finite element method in their computations whereas other groups [29] use spectral element discretization techniques. An arbitrary Lagrangian-Eulerian (ALE) methodology is usually employed to handle moving boundaries wherein moving/deformable grids are employed. These methods offer great flexibility for modeling of flow with complex moving boundaries. However, remeshing algorithms can significantly increased the complexity of the solution procedure and can sometimes compromise the robustness and accuracy of the solution procedure.

B.2 Cartesian grid methods

In recent years, a new approach has come to fore which is well suited for simulating flows with complex moving boundaries. In 1970's Peskin introduced his "immersed boundary method" which is used to simulate flow in a modeled human heart [30,31]. The key feature of this method was that simulations with complex moving boundaries were carried out on stationary Cartesian grids and this eliminated the need for complicated remeshing algorithms that are usually employed with conventional body-conformal methods. Since then a number of different variations of this methods have been developed including the front tracking method [32], immersed-interface methods [33] cut-cell Cartesian grid method [34-36], fictitious domain method [37] and ghost fluid method [38]. These methods have been used to solve a large variety of flows with complex moving boundaries including cardiovascular flows [31], multiphase flows [32,38], fluid-structure interaction [39,40], fluid machinery [41], micro-fluidic devices [42], biological locomotion [43] and flapping foils [44].

These methods provide a unique capability for simulating flow with complex moving boundaries and as such, are ideally suited for simulation of bio-hydrodyanmic flows. In a later section we will show computed results for a configuration involving two flapping foils where the computations have been performed using a Cartesian grid method. Figure 9 shows an example of a Cartesian grid with local refinement that could be uses to simulate the airfoil flow.

III. Application to Bio-Hydrodynamics

A. Two-Dimensional Flapping Foils

A number of groups have employed numerical simulations to investigate the hydrodynamics of flapping foils. Chief among these are the groups at the U.S. Naval Postgraduate School [4-6,15], and NRL (Ramamurti & Coworkers). Both groups have employed Euler as well as RANS codes for analysis of flapping foils but here we focus primarily on the RANS calculations. Another RANS study that will be discussed in detail here is that of Isogai et al. [46]. For the following discussion consider a simple pitch and plunge (or heave) motion of a foil prescribed as follows:

$$h = h_1 \sin(2\pi f t);$$

$$\alpha = \alpha_o + \alpha_1 \sin(2\pi f t + \phi)$$

where h_1 is the plunge (or heave) amplitude, α_o is the mean pitch angle and α_1 is the amplitude of the sinusoidal pitch angle variation. Furthermore, f is the flapping frequency and ϕ is the phase difference between the pitch and plunge motions. In addition to α_o, α_1 and ϕ, the non-dimensional parameters that govern the fluid dynamics of this configuration are normalized plunge amplitude $h_1^* = h_1 / c$, the Reynolds number $\mathrm{Re}_\infty = U_\infty c / \nu$ (where U_∞ is the freestream velocity, c is the foil chord and ν is the kinematic viscosity of the fluid) and the Strouhal number $St = 2fh_1 / U_\infty$ based on the wake width [45]. An alternative frequency parameter based on the foil chord $k = 2\pi fc / U_\infty$ has also been used in a number of studies [15, 46]. Note that $kh_1^* = \pi St$, and this product is also equal to the peak plunge velocity normalized by the freestream velocity.

It should be noted that a complete numerical investigation of the parameters space of even this simple flapping foil configuration has yet to be undertaken. However, recent RANS simulations of Tuncer & Platzer [15], when put together with those of Isogai et al. [46] represent the most comprehensive numerical evaluation of this configuration and we discuss the salient results from these studies. Both Isogai et al [46] and Tuncer & Platzer [15] employ a NACA 0012 foil and solve the Reynolds averaged compressible Navier-Stokes equations on a structured grid. Tuncer's code employs a 3rd-order upwind-biased scheme in space whereas Isogai's code employs a TVD scheme. Both codes use the Baldwin-Lomax turbulence model. As in most RANS calculations, a fine mesh is employed near the body but away from the body, the mesh is coarsened and the numerical viscosity is allowed to dissipate the vortex structures. Table 1 summarizes the range of parameters examined in these studies and following figures show a sampling of the data obtained from these simulations.

Figure 10 shows the effect of flapping amplitude and frequency on the thrust produced by the foil. These are two parameters that are known to have a significant effect on the thrust and this is confirmed by these computations. Replotting of the same data against the Strouhal number leads to a better collapse, which is inline with the findings of Triantafyllou et al. [45].

Figure 11 shows the variation in thrust coefficient and efficiency for a foil undergoing combined pitch and heave and trends are similar to those observed by Anderson et al. [7] . In both computational studies, larger values of pitch amplitude have not been examined. Tuncer and Platzer [15] indicate that the solver has convergence problems for high pitch

amplitudes. This might possibly be due to inadequate resolution of the large-scale dynamic stall vortices that form at high pitch amplitudes.

The final plot (fig. 12) shows the effect of varying the phase angle between pitch and plunge on the thust and efficiency. The trend that emerges here, i.e. maximal thrust and efficiency at a phase angle of about roughly 90^o is also well established in experiments [3,7]. It is interesting to note that these two studies employ very similar computational methodologies and simulate precisely the same configuration. Furthermore both indicate that the results are grid independent. However, despite this, the resulting thrust and efficiencies for some cases differ by over 30%. As noted by both groups in their respective papers, the cause for this discrepancy is not clear. In our view, this clearly indicates that simulation fidelity is not guaranteed by grid independence in these RANS computations and turbulence modeling effects have to be examined.

Ramamurti et al [47] have also simulated a similar configuration (NACA 0012 foil undergoing pitch and heave motion in a freestream). However, Ramamurti et al. solve the incompressible Navier-Stokes equations on an unstructured grid, which is significant departure from these other simulations. A relatively complex mesh movement algorithm is employed which allows for the generation of a body-conformal mesh at every time-step. The solver has been used to study the foil in pitch only as well as combined pitch and heave. Figure 13 (a) shows a comparison of computed data for the 2^o pitch oscillation case with experiments of Koochesfehani [48]. As pointed out by the authors, there is significant mismatch between the experiments and computations at higher frequencies. Ramamurti and Sandberg [47] make a convincing case that the discrepancy is due to inaccuracies in measuring the thrust in the experiment. In experiments, thrust is usually estimated by extracting the mean velocity downstream of the foil and estimating the increase in momentum flux in the wake. Since this discounts the contribution of mean pressure and velocity fluctuations on the momentum balance, this method is accurate only if the measurements are made far enough downstream of the foil where the pressure has recovered to freestream values and the velocity fluctuations are small. Also shown in the adjoining figure (13b) are the computed results of the foil in pitch and heave motion where the configuration is similar to that of the experiments of Anderson [49]. The plot shows the variation of thrust with change in phase angle between the pitch and heave motions and the computed results are found to be generally consistent with the experiments.

It would seem that we now have a relatively good understanding of the effect of the frequency (St or k), amplitude (h_1^*) and pitch and heave phase difference (ϕ) on the hydrodynamic performance of 2D flapping foils. The effect of the Reynolds number on the foil performance is somewhat less well understood. Most simulations and experiments of flapping foils have been carried out in the subcritical ($Re<10^6$) regime [5,15,46,50]) since this is the range relevant to the swimming of small fish. Within this subcritical range, the general trend is that thrust increases with Reynolds number [50]. However, from an engineering point of view, it might be useful to understand the operation of flapping foils at postcritical Reynolds numbers ($Re>10^6$) since AUVs (such as REMUS) often operate in this regime. The effect of α_o on the foil performance is also not well understood. Since the primary effect of α_o is on the transverse (lift) force and not the thrust, past studies, which have focused mainly on propulsion and not maneuvering, have tended to disregard this parameter. A non-zero value of α_o could produce significant magnitudes of transverse force which could be used in turning, pitching as well as rolling maneuvers. There have been some experimental studies that have examined the effect of this parameter [51-53]. In a study of hover modes by Freymuth [51], it was shown that the angle of the hover jet (and therefore the direction of the thrust vector) could be manipulated quite easily using this parameter. Further understanding of this parameter is however needed, especially with regard to its effect on the hydrodynamic forces.

Also, hover modes (for which $U_\infty = 0$), which are relevant to low-speed maneuvering hydrodynamics, have also not been examined extensively. In addition to the experimental work of Freymuth [51,54], hover modes for 2D foils have been examined by Gustafson and Leben [55] , Wang [56] and Mittal et al. [44]. One key finding from the study of Wang [56] was the rapid increase in the hydrodynamic force with h_1^* upto about h_1^*=2, beyond which the force was relatively insensitive to the plunge amplitude. This result is inline with the findings of Freymuth [51]. Mittal et al. [44] simulated the flow associated with an elliptic airfoil in hover. The primary variable in their study was α_1 which was varied from 30^o to 75^o. The simulations indicated that variation in the pitch amplitude produced a range of wake topologies (see figure 14). For $\alpha_1 = 45^o$, an inverse Karman vortex street was generated and this was associated with optimal thrust production as estimated by the ratio of the mean thrust and the root-mean-square transverse force (see figure 15).

This brings us to the next aspect that the RANS computations have not yet addressed systematically, which is, the role of wake topologies on the foil performance. Experiments clearly show that vortex dynamics in the wake oftentimes holds the key to the performance of flapping foils [2,44,48,49,51,49]. However, as pointed out earlier, the RANS approach does not lend itself naturally to simulation and analysis of wake topologies. Flow separation which usually precedes the formation of the wake, is not easily predicted using RANS. Most RANS computations coarsen the grid rapidly away from the wall and in the wake, and rely on numerical dissipation to damp out the vortex structures. Tuncer & Platzer [15] have attempted to use Lagrangian tracers in conjunction with their RANS computations to

visualize the wake topology and provide some qualitative validation of their computational methodology. However, direct visualization of the wake topology through an adequately resolved vorticity field is highly desirable and DNS, LES and DES type techniques are well suited for this purpose.

Most past studies of flapping foils, due to their focus on propulsion, have primarily limited themselves to understanding the dependence of mean thrust and efficiency on the foil parameters. However, the magnitude of oscillatory components of both the thrust and transverse (lift) force on the foil can often be significantly larger than the mean values. Due to their large magnitudes, these oscillatory components could significantly affect the dynamics and control of an AUV powered by flapping foils. It is therefore crucial to parameterize the oscillatory components of force in addition to the mean components.

Finally, the focus of past studies has primarily been on foils undergoing flapping motion. However, as discussed by Walker & Westneat [57], flapping motion is relevant for energy efficient operation such as required during cruising, whereas rowing is more relevant to slow speed, maneuvering (starting, stopping, yawing etc.) motion. Recent blade-element computations of Walker and Westneat [57] indicate that even though flapping motion is more efficient at all flow speeds, higher thrust can be generated at low speed through a rowing motion. Interestingly, the simulations of Walker & Westneat [58] indicate that the optimal reduced frequency ($k = \omega C / 2U_\infty$) for rowing with a fully feathered recovery stroke is roughly the same as the flapping stroke. Since the optimality of the flapping stroke has been connected to the wake topology [7], similar flow features probably occur for optimal rowing motion as well. However, little is known about the wake topologies for fins undergoing a rowing motion and this aspect could be easily investigated through viscous flow simulations.

B. Three-Dimensional Flapping Foils

We focus now on computations of 3D flapping foil which have more relevance in the context of low-speed maneuvering biohydrodynamics. For such foils, the aspect-ratio (*AR*) defined as $(\text{span})^2/(\text{area})$ also has to be considered. It should be noted that many highly maneuverable fish have relatively low aspect ratio fins. For instance, mean aspect ratio values of the pectoral, dorsal and anal fins for a boxfish *Ostracion meleagris* have been measured to be 1.9, 1.5 and 1.7 respectively [60] and those of a striped surfperch were found to be in the 1.8-2.5 range [61]. Furthermore, fish fins usually have highly complex, three-dimensional planforms. There are relatively few computational studies of 3D flapping foils primarily because such computations tend to be highly complex and expensive. Liu & Kawachi [62] were one of the first to perform viscous flow computations of 3-D flapping foils. The configuration chosen in this study attempted to match the experiments of Van den Berg and Ellington [63]. In this experiment, a mechanical flapper was used to study the fluid dynamics of a hawkmoth wing which had a relatively complex three-dimensional planform. The Reynolds number (Re) and frequency parameter (*k*) were 4000 and 0.74 respectively and a relatively coarse mesh with 72,000 points was used. The computations were validated qualitatively by comparing with the smoke visualizations of Van den Berg and Ellington [63]. The computational study was used to examine the role of leading edge vortices on the force production. In a similar vein, Ramamurti et al. [8] have simulated the flow generated by a three-dimensional foil in hover where the flow configuration matches the *Drosophila melanogaster* wing experiments of Dickinson et al. [64]. These computations are primarily inviscid although, interestingly, comparisons with viscous simulations seem to indicate that viscous effects are not significant [8]. Computations are validated quantitatively by comparing computed forces against experimental measurements. The study examines the effect of phasing between translational and rotational motions and confirms the findings of Dickinson et al. [64] that rotational mechanisms play an important role in the production of hydrodynamic forces.

Perhaps the most ambitious simulations of 3D flapping foils to date are those of the bird wrasse pectoral fin by Ramamurti et al. [65], which attempt to match the experiments of Walker & Westneat [59]. The pectoral fin kinematic data extracted from the experiments has been used to develop a realistic computational model of the 3D flexible pectoral fin. Steady, quasi-steady and unsteady viscous flow computations have been carried out and the computed hydrodynamic forces correlated with the formation of flow structures in the vicinity of the pectoral fin. Since no detailed fluid flow measurements were made for the swimming fish in the experiment of Walker & Westneat [59] strong validation of the computations could not be provided.

As demonstrated by the above-mentioned studies, a comprehensive computational analysis of the fluid dynamics of 3-D flapping foils is quite feasible on current generation computers. Simulation of realistic and highly complex configurations such as the bird wrasse by Ramamurti et al. [65] certainly point to the growing role that computational modeling will play in bio-hydrodynamics. However, due to the many complex features that are simultaneously included in these models, it is generally quite difficult to extract clear insight into the underlying flow mechanisms and to delineate flow features/mechanisms that are universal from those that are specific to a particular configuration. Therefore a program of computations that systematically examines the effect of the key 3D parameters on the foil performance would go a long way towards improving our understanding of these flows.

Key parameters that need to be considered are the foil aspect ratio and the foil planform. Recent DPIV experiments of live swimming fishes by Drucker & Lauder [2] indicate that vortex rings are a dominant feature in the pectoral fin wake (see figure 16). It would therefore be of interest to examine wake topologies of 3D flapping foils and connect these wake

topologies to optimal thrust conditions as has been done for 2D flapping foils [7]. The fin planform is also an important factor for 3D flapping foils and recent experiments [57,66,67], have examined the correlation of fin shape with performance. The experiments of Combes & Daniel [66] with a spotted ratfish (*Hydrolagus colliei*) suggest that the aspect ratio as well as the proportion of area in the outer one-fifth of the wing can characterize the hydro-dynamics performance of the flapping fin. Computational modeling is ideally suited for examining this issue further since confounding variables can be effectively eliminated in these models, thereby allowing us to isolate the effect of planform on the foil performance.

C. *Effect of Fin Flexion*

Fins of most small, highly maneuverable fish tend to be highly flexible. Fin flexion, when controlled actively, allows for on-demand morphing of the fin and can provide exquisite control over a large operational envelope. Interestingly, the quest for a similar capability forms the basis for the NASA Morphing Project (http://www.dfrc.nasa.gov/PAO/X-Press/stories/043001/new_morph.html). The recent study of Combes and Daniel [66] indicates that flexion in the pectoral fin of a ratfish reduces the thrust and increases the efficiency. Apart from this, little work has been done to understand the penalties/benefits of fin flexion. This issue is another one that is well suited for investigation through computational modeling. In computational models, flexion can be varied in a systematic manner in order to examine its effect on fin performance. Inclusion of flexion would require a two-way coupled solution procedure and would have to incorporate an appropriate constitutive model for the fin material. An example of such an approach is the work of Shyy et al. [68] who have used numerical simulations to compare the aerodynamic performance of flexible and rigid membrane wings.

D. *Full-Body Hydrodynamics*

The presence of the body can potentially have a significant effect on locomotor performance especially during maneuvering motions. However, relatively little work has been done in using numerical simulations to study the full-body hydrodynamics. In a first-of-its-kind effort, Liu et al. [50] studied undulatory locomotion of a tadpole using viscous flow simulations. Ramamurti et al. [65] have simulated flow past a bird wrasse with a flapping pectoral fin. However, the focus of the study was on the pectoral fin and not the flow over the body. The issue of body-fin interaction therefore remains open and needs to be investigated through simulations and experiments. Due to the computational costs associated with simulating full body hydrodynamics, RANS and DES seem best suited for this purpose. These modeling techniques can be used to identify critical regions in the parameter space which can then be subjected to detailed study through LES and DNS.

E. *Biologically Inspired Active Control*

This is another area that is of importance in biomimetic hydromechanical systems. Consider for example the bluegill sunfish (Figure 17) that has been the subject of investigation by Drucker & Lauder [2]. Based on DPIV data, Drucker and Lauder have hypothesized that vortex structures shed by the soft dorsal fin could enhance the thrust of the tail fin. This hypothesis has been examined through 2D numerical simulations by Akhtar et al [69]. Kinematic data from the experiments (Figure 18) has been used to set up a simulation of flow past two flapping foils so as to mimic the interaction of the soft-dorsal and tail fins. These simulations employ a Cartesian grid method [35,39] wherein the simulations are carried out on a stationary Cartesian grid.

Figure 19 shows a qualitative comparison of the experimental and computational flow visualizations. Thrust and efficiency of the tail fin with and without the upstream soft-dorsal fin has been computed and compared. In the 2D simulations, the thrust and efficiency of the tail fin is found to increase by about 100% and 50% respectively, thereby providing strong support to the hypothesis of Drucker & Lauder [2]. The simulations indicate that the vortex structures from the dorsal fin increase the apparent pitch angle of the tail fin at mid-stroke (see figure 20). This leads to the formation of a large leading edge vortex that stays attached to the fin and increases the thrust on the foil.

The simulations also indicate that the thrust and efficiency can be augmented further by reducing the phase lag between the two fins, which may be considered analogous to reducing the gap between the fins. On the other hand, increase in phase lag (which may be interpreted as increasing the gap between the fins) can reduce the tail fin performance below nominal levels. A survey shows that a number of different species of fish exhibit the presence of fin structures that are located on the midline between the main dorsal and caudal fins. The adipose fin, which is found in many early teleosts including salmonids is one such example. Figure 21 shows the structure and location of this fin. This non-rayed fin is considered a vestigial organ by some, whereas others have conjectured that this fin might increase the stability of the fish. However, the work of Akhtar et al. [69] also raises the possibility that the vortex structures produced by these types of appendages could increase the thrust of the tail fin. As has been demonstrated by Akhtar et al. [69], this issue can be investigated in a comprehensive manner by using numerical simulations. Such thrust augmentation strategies could potentially have large payoffs in engineered biomimetic systems where even small increases in efficiency could translate to larger payloads and/or extended operational envelope.

F. *Biologically Inspired Control Surfaces*

Control surfaces found on some swimming animals exhibit features which could confer distinct hydrodynamic advantages. Two examples are the humpback whale flipper and the cephalofoil of the hammerhead shark. The remarkable hydrodynamic design of the flipper of a humpback whale has been examined in detail by Fish and Battle [70]. They have

suggested that the tubercles (Figure 22a) act as leading edge vortex generators that can prevent/delay stall and thereby maintain a large lift-to-drag ratio at high angles of attack. Watts and Fish [9] have used a panel method to examine the performance of a foil with and without leading edge tubercles at 10^o angle-of-attack and these computations show that the presence of the tubercles can increase the lift by about 5%, reduce drag by 11% and increase the lift-to-drag ratio by about 18%. Viscous flow simulation along the same lines could be used to further understand the underlying flow mechanisms especially at higher angles-of-attack where the predictive capability of panel method deteriorates significantly. The cephalofoil of some species of hammerhead sharks also shows characteristic scalloping on the leading edge (see figure 22b). Although little is know regarding the hydrodynamic function of these leading edge structures, it seems plausible that they produce an effect similar to the tubercles on a humpback flipper.

IV. CONCLUSIONS

Computational modeling and simulation of bio-hydrodynamic flows is still in its infancy. Computational modeling gives us the ability to eliminate confounding variables and isolate effects and mechanisms associated with chosen parameters. Computations also provide detailed full field information about the flow. Due to this, it is expected that computational modeling will play an increasing role in the analysis of these flow configurations in the future. In addition to inviscid and RANS modeling that has been the norm in this area, it is expected that more accurate modeling techniques such as DES, LES and DNS will also be brought to bear on these problems. These techniques provide significantly more information about the flow, which is essential for understanding the flow physics. Cartesian grid methods are also expected to find a wide use in computational modeling of bio-hydrodynamic configurations. Systematic and comprehensive validation remains a crucial component of these computational investigations and requires that quantitative fluid flow data, such as that extracted from DPIV [2], be available from experiments.

Following key areas/issues in bio-hydrodynamics have been identified where progress could be made using computational modeling:

- Further parameter survey of 2D flapping foils.
- Parameterization of oscillatory components of forces on flapping foils.
- Performance and wake topologies of 3D foils including systematic investigation of aspect-ratio and planform effects.
- Examination of hovering and rowing motions, which are relevant to low-speed maneuvering bio-hydrodynamics.
- Penalties/benefits of fin flexion.
- Biologically inspired control surfaces and active control strategies.

REFERENCES

[1] Triantafyllou M. S. and Triantafyllou S An efficient swimming machine," Scientific American, 272, pp. 64-70 1995.

[2] Drucker E. and Lauder V. 2002 Experimental hydrodynamics of fish locomotion: functional insights from wake visualization. Integ. and Comp. Biol. 42:243-257.

[3] Katz, J. and Weihs, D. 1978 Hydrodynamic propulsion by large amplitude oscillations of an airfoil with chordwise flexibility. J. Fluid Mech. 88, 485-497.

[4] Jones, K. D., Lai, J. C. S., Tuncer, I. H. and Platzer, M. F. 2000. Computational and Experimental Investigation of Flapping-Foil Propulsion Presented at the 1st International Symposium on Aqua Bio-Mechanisms / International Seminar on Aqua Bio-Mechanisms, Tokai University Pacific Center, Honolulu, Hawaii, August 27-30, 2000.

[5] Jones, K. D., Castro, B. M., Mahmoud, O. and M.F. Platzer 2002. Numerical and Experimental Investigation of Flapping-Wing Propulsion in Ground Effect AIAA 2002-0866, Presented at the AIAA 40th Aerospace Sciences Meeting, Reno, Nevada, January 14-17, 2002.

[6] Jones, K. D. and Platzer, M. F. 2002. On the design of efficient micro air vehicles. Design and Nature Comparing Design in Nature with Science and Engineering, Press, Eds. Brebbia, C.A., Sucharov, L.J. and Pascolo, P., WIT Press, Southampton, UK, 2002, pp. 67-76.

[7] Anderson, J. M., Streitlien, K., Barrett, D. S. and Triantafyllou, M.S. 1998 Oscillating Foils of High Propulsive Efficiency. J. Fluid Mech. 360:41-72.

[8] Ramamurti, R. and Sandberg, W. C. 2002. A Three-Dimensional Computational Study of the Aerodynamic Mechanisms of Insect Flight, J. Exp. Biol., Vol. 205, No. 10, pp. 1507-1518.

[9] Watts P. & Fish, F.E. 2001 The influence of passive, leading edge tubercles on wing performance. In. Proc. 12th Int. Symo. Unmanned Untethered Submesible Technolody, Autonomous Undersea Systems Institute, Durham, New Hampshire.

[10] Lan, C. E., 1979 The Unsteady Quasi-vortex-lattice Method with Applications to Animal Propulsion, J. Fluid Mech., vol. 93, part 4, pp. 747-765.

[11] Smith, M. J. C. 1996 Simulating moth wing aerodynamics: towards the development of flapping-wing technology. AIAA Journal, 34(7) pp 1348-1355.

[12] Wilcox, D.C. 1998 Turbulence Modeling for CFD, DCW Industries.

[13] Baldwin, B.S. and Lomax, H. 1978 Thin layer approximation and algebraic model for separated turbulent flow. AIAA 78-757.

[14] Spalart, P. R., Jou, W. H., Strelets, M., and Allmaras, S. R. (1997) "Comments on the Feasibility of LES for Wings, And on a Hybrid RANS/LES Approach," First AFOSR International Conference On DNS/LES, Aug. 4-8, 1997, Ruston, Louisiana. In Advances in DNS/LES, Liu, C., and Liu, Z., eds., Greyden Press, Columbus, Ohio

[15] Tuncer, I. H. and Platzer, M. F. 2000. Computational Study of Flapping Airfoil Aerodyanmics. AIAA Journal of Aircraft, Vol. 37, No.3 May-June 2000, pp. 514-520.

[16] Piomelli, U. Large-eddy simulation: achievements and challenges. Progress in Aerospace Sciences, 1999, 35, 335-362.

[17] Karniadakis E. & Triantafyllou, S. 1992 ``Three-dimensional dynamics and transition to turbulence in the wake of bluff objects," J. Fluid Mech., vol. 238, p. 1.

[18] Mittal, R Wilson, J J Najjar F M 2002. Symmetry properties of the transitional sphere wake.. AIAA Journal Vol 40, No 3.

[19] Mittal R. & Balachandar S. 1995 Effect of Three-Dimensionality on the Lift and Drag of Nominally Two-Dimensional Cylinders Phys. Fluids, Vol. 7(8) 1841-1865.

[20] Newman, J. and Karniadakis, E. Simulations of flow past a freely vibrating cable. Journal of Fluid Mechanics, 1997, 344, 95.

[21] Baggett, J. S., Jimenez, J. & Kravchenko, A. 1997 Resolution requirements in large-eddy simulations of shear flows. Annual Research Briefs, Center for Turbulence Research, NASA Ames/Stanford Univ. 51-66.

[22] Kaltenbach, H-J., Fatica, M., Mittal, R., Lund, T.S. and Moin, P. Study of flow in a planar asymmetric diffuser using large-eddy simulation. Journal of Fluid Mechanics, 1999, 390, 151-186.

[23] You, D., Mittal, R., Wang, M. and Moin, P. Progress in large-eddy simulation of a rotor tip-clearance flow. 12th Annual DoD HPCMP User Group Conference, 2002, Austin, TX.

[24] Muthanna, C, Wittmer K S and Devenport W J, "Turbulence structure of the flow downstream of a compressor cascade with tip leakage", AIAA 36th Aerospace Sciences Meeting, Reno, Nevada, January 1998. AIAA 98-0420.

[25] Germano, M., Piomelli, U., Moin, P., and Cabot, W. H. (1991). A dynamic sub-grid scale eddy viscosity model. Phys. Fluids, A(3):1760-1765.

[26] Squires, K. D., Forsythe, J. R., Morton, S. A., Strang, W. Z., Wurtzler, K. E., Tomaro, R. F., Grismer, M. J. and Spalart. P. R. 2002. Progress on Detached-Eddy Simulation of massively separated flows'AIAA Paper 2002-1021.

[27] Chan, W. M. and Meakin, R. L., 1997 "Advances Towards Automatic Surface Domain Decomposition and Grid Generation for Overset Grids," AIAA Paper 97-1979, in Proceedings of the AIAA 13th Computational Fluid Dynamics Conference, Snowmass, Colorado.

[28] Ramamurti, R. and Sandberg, W. C. 2002. A Three-Dimensional Computational Study of the Aerodynamic Mechanisms of Insect Flight, J. Exp. Biol., Vol. 205, No. 10, pp. 1507-1518.

[29] Karniadakis E. & Sherwin, S.J. 1999``Spectral/hp Element Methods for CFD," Oxford University Press, March.

[30] Peskin, C.S. Numerical analysis of blood flow in the heart, Journal of Computational Physics, 1977, 25, 229-252.

[31] Peskin, C. S. and McQueen, D. M. 1989. A three-dimensional computational model of blood flow in the heart I. immersed elastic fibers in a viscous incompressible fluid. Journal of Computational Physics, 81:372-405.

[32] Tryggvason, B. Bunner, O. Ebrat, and W. Tauber. Computations of Multiphase Flows by a Finite Difference/Front Tracking Method. I Multi-Fluid Flows. In: 29th Computational Fluid Dynamics. Lecture Series 1998-03. Von Karman Institute for Fluid Dynamics.

[33] Leveque, R.J. and Li, Z. 1994 The Immersed interface method for elliptic equations and discontinuous coefficients and singular sources. SIAM J. Numer. Anal. 21, 101-9.

[34] Ye, T., Mittal, R., Udaykumar, H.S. and Shyy, W. An accurate Cartesian grid method for simulation of viscous incompressible flows with complex immersed boundaries. Journal of Computational Physics, 1999, 156, 209-240.

[35] Udaykumar, H.S., Mittal, R., Rampunggoon, P. and Khanna, A. A sharp interface cartesian grid method for simulating flows with complex moving boundaries. Journal of Computational Physics, 2001, 174, 345-380.

[36] Udaykumar, H.S. Mittal, R. and Rampunggoon, P. Interface tracking finite volume method for complex solid-fluid interactions on fixed meshes. Communications in Numerical Methods in Engineering, 2002, 18, 89-97.

[37] Glowinski, R.. Pan, T.W Periaux, J. 1996. Fictitious domain methods for the simulation of Stokes flow past a moving disk , in Computational Fluid Dynamics J.A. Desideri, C. Hirsh, P. Le Tallec, M. Pandolfi, J. Periaux eds., John Wiley & Sons, Chichester, England, 64-70.

[38] Fedkiw, R. and Liu, X.-D.,"The Ghost Fluid Method for Viscous Flows",Innovative Methods for Numerical Solutions of Partial Differential Equations, edited by M. Hafez and J.-J. Chattot, pp. 111-143, World Scientific Publishing, New Jersey, 2002.

[39] Mittal, R., Seshadri, V., Sarma, S. and Udaykumar, H.S. Computational modeling of fluidic micro-handling processes. Fifth International Conference on Modeling and Simulation of Microsystems, San Juan, Puerto-Rico, 2002.

[40] Mittal, R., Bonilla, C. and Udaykumar, H.S. 2003 Cartesian Grid Methods for Simulating Flows with Moving Boundaries. To appear in Proceedings of Eleventh International Conference on Computational Methods and Experimental.

[41] Fadlun, E.A., Verzicco, R., Orlandi, P. & Mohd-Yusof, J. ``Combined immersed-boundary/finite-difference methods for three-dimensional complex flow simulations" J. of Comp. Phys., 161, (2000), 35-60

[42] Mittal, R. and Rampunggoon, P. On the virtual aero shaping effect of synthetic jets. Physics of Fluids, 2002, 14, 1533-1536.

[43] Fauci, L.J. and Peskin, C.S. 1988 A computational model of aquatic animal locomotion. J. Comput. Phys. 77, 85-108.

[44] Mittal, R., Utturkar, Y. and Udaykumar, H.S. Computational modeling and analysis of biomimetic flight mechanisms. AIAA 2002-0865. 40th Aerospace Sciences meeting and Exhibit, Reno, NV. January 2002.

[45] Triantafyllou, S., Triantafyllou, M. S. and Grosenbaugh, M. A. 1992 Optimal thurst development in oscillating foils with applications to fish propulsion. J. of Fluids and Structures 7, 205-224.

[46] Isogai, K., Shinmoto, Y. and Watanabe, Y. 1999 Effects of Dynamic Stall on Propulsive Efficiency and Thrust of Flapping Airfoil," AIAA Journal, Vol.37, No.10, pp 1145-1151.

[47] Ramamurti, R., Sandberg, W. C. and Löhner, R. 2001. Simulation of Flow About Flapping Airfoils Using a Finite Element Incompressible Flow Solver. AIAA J., Vol. 39, No. 2, pp. 253-260, 2001.

[48] Koochesfahani. M. M. 1987 Vortical Patterns in the Wake of an Oscillating Airfoil Presented as paper 87-0111 at the AIAA 25th Aerospace Sciences Meeting, Reno, NV, Jan. 12-15.

[49] Anderson, J.M. 1996 PhD Thesis.

[50] Liu, H. and Kawachi, K. 1999 A Numerical Study of Undulatory Swimming, Journal of Computational Physics, 155:223-247.

[51] Freymuth P. 1990 Thrust generation by an airfoil in hover modes. Expts Fluids, 9:17-24.

[52] Ohmi, K., Coutanceau, M., Loc, T.P. & Dulieu, A. 1990. Vortex formation around an oscillating and translating airfoil at large incidences. J. Fluid Mech. 211, 37-60.

[53] Ohmi, K., Coutanceau, M., Daube, O. and Loc, T.P. 1991 Further Experiments on oscillating and translating airfoil at large incidences. J. Fluid Mech, 225, 607-630.

[54] Freymuth, P. 1988 Propulsive Vortical Signature of Plunging and Pitching Airfoils, AIAA J. 26 No. 7, pp 881-883.

[55] Gustafson, K. E. and Leben, R. 1991 Computation of dragonfly aerodynamics. Computer Physics Comm. 65:121-132.

[56] Wang, Z.J. 2001 Two dimensional mechanism for insect hovering. Phys. Rev. Lett. Vol 85, No. 10, 2216-19.

[57] Walker, J.A and Westneat, M.W. 2002 Performance limits of labriform propulsion and correlates with fin shape and motion. Journal of Experimental Biology 205:177-187.

[58] Walker, J.A. and Westneat, M. W. 2000 Mechanical performance of aquatic rowing and flying. Proceedings of the Royal Society of London, Series B, 267:1875-1881.

[59] Walker, J.A. and Westneat, M. W. 1997. Labriform propulsion in fishes: Kinematics of flapping aquatic flight in the bird wrasse, Gomphosus varius (Labridae). J. of Experimental Biology, 200:1549-1569.

[60] Hove, J. R., O'Bryan, L. M., Gordon, M. S., Webb, P. W. and Weihs, D. 2001. Boxfishes (Teleostie: Ostraciidae) as a model system for fishes swimming with many fins: I. Kinematics. J. exp. Biol. 204: 1459-1471.

[61] Drucker, E. and Jensen, J. S. 1997. Kinematic and electromyographic analysis of steady pectoral fin swimming in the surfperches. J. of Experimental Biology 200:1709-1723.

[62] Liu, H. and Kawachi, K. 1998 A Numerical Study of Insect Flight, Journal of Computational Physics, 146:124-156.

[63] Van den Berg, C. and Ellington, C.P. 1997 The vortex wake of a `hovering' model hawkmoth. Phil. Trans. R. Soc. Lond. B. 352, 317-328.

[64] Dickinson, M. H., Lehmann, F. O. and Sane, S. P. 1999 Wing Rotation and the Aerodynamic Basics of Insect Flight. Science 284:1954-1960.

[65] Ramamurti, R., Sandberg, W. C., Löhner, R., Walker, J. A. and Westneat, M. W. 2002 Fluid dynamics of flapping aquatic flight in the bird wrasse: 3-D unsteady computations with fin deformation. Journal of Experimental Biology, 205:2997-3008.

[66] Combes, S.A. and Daniel, T.L. 2001 Shape, Flapping and Flexion: Wing and Fin design for forward flight. J. Exp. Biol. 204, 2073-2085.

[67] Wainwright, P.C., Belowood, D. R. and Westneat, M. W. 2002 Pectoral fin diversity in labrid fishes. Env. Biol. Fish (in press).

[68] Shyy, W., Jenkins, D. A. and Smith, R.W. Study of adaptive shape airfoils at low Reynolds numbers in oscillatory flow. AIAA J. 1997; 35, 154501548.

[69] Akhtar, I., Mittal, R. and Lauder, V. Thrust augmentation through active flow control: lessons from a bluegill sunfish. Bulletin of American Physical Society, 2002, 52nd APS DFD meeting, Dallas.

[70] Fish, F. E. and J. M. Battle. 1995. Hydrodynamic design of the humpback whale flipper. Journal of Morphology, 225:51-60.

Figure 1. Bluegill sunfish (Picture courtesy G.V. Lauder)

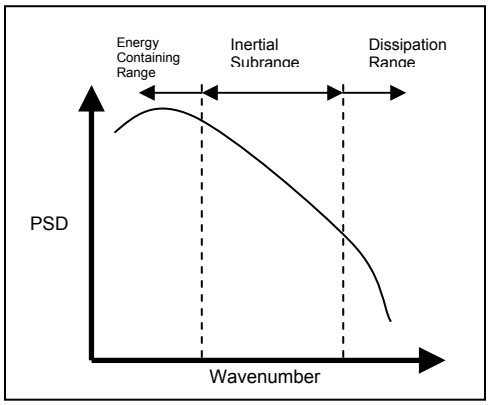

Figure 2. Typical energy spectra for a turbulent flow showing the various ranges.

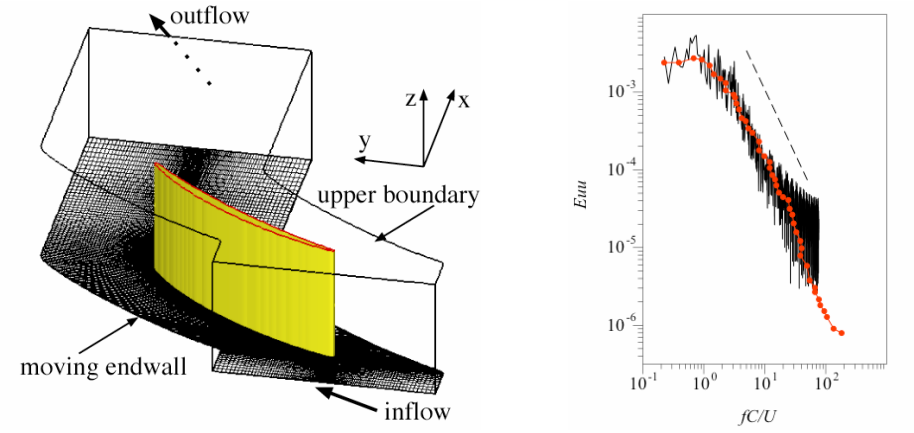

(a) (b)

Figure 3 (a) Rotor tip flow configuration being computed using LES in You et al [23]. (b) Comparison of computed (solid line) and experimental (red dot) power spectra.

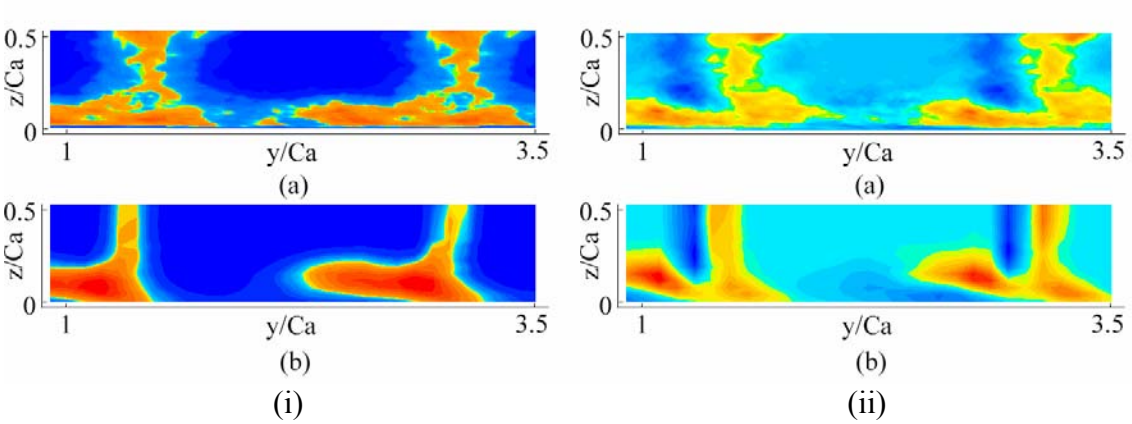

Figure 4 Comparison of computed (a) and experimental (b) Reynolds stresses downstream of the blade by You et al. [23] (i) $\langle u'v' \rangle$ (ii) $\langle v'^2 \rangle$

-

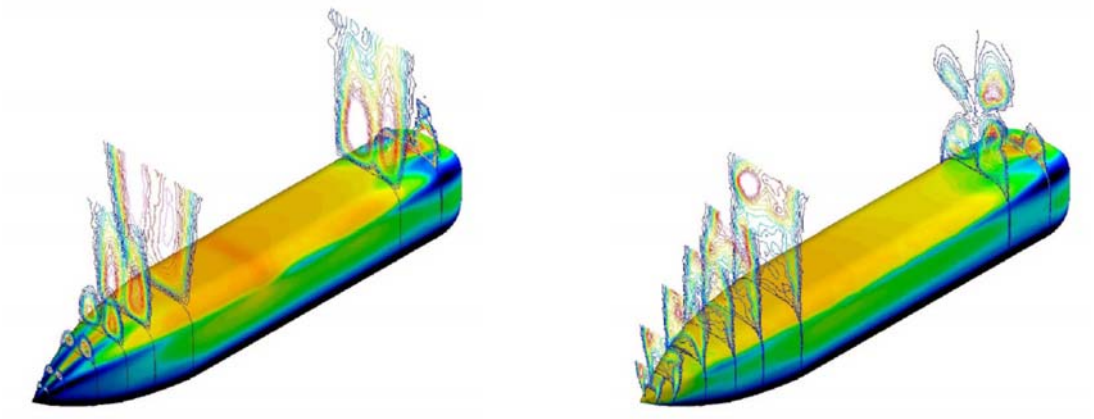

Figure 5. Comparison of wake topology for RANS (a) and DES (b) computations of flow over a forebody by Squires et al. [26]

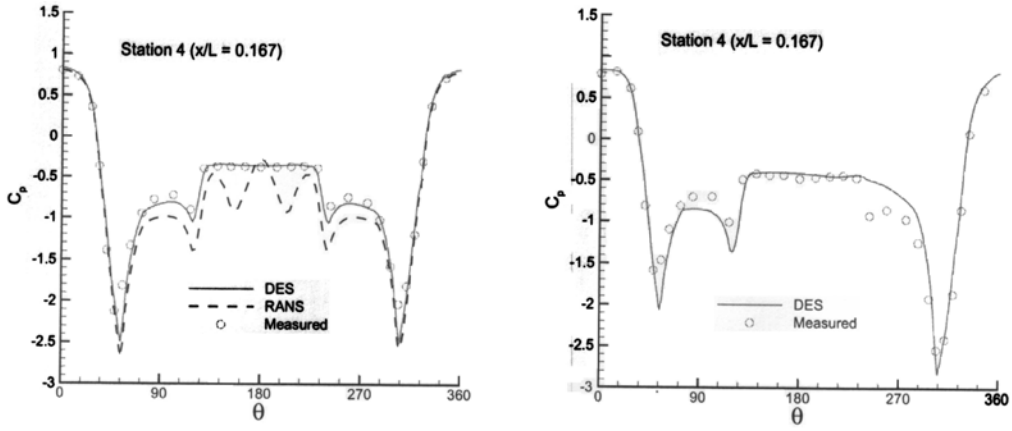

Figure 6. Comparison of surface pressure between RANS, DES and experiments for the forebody flow from Ref. 26.

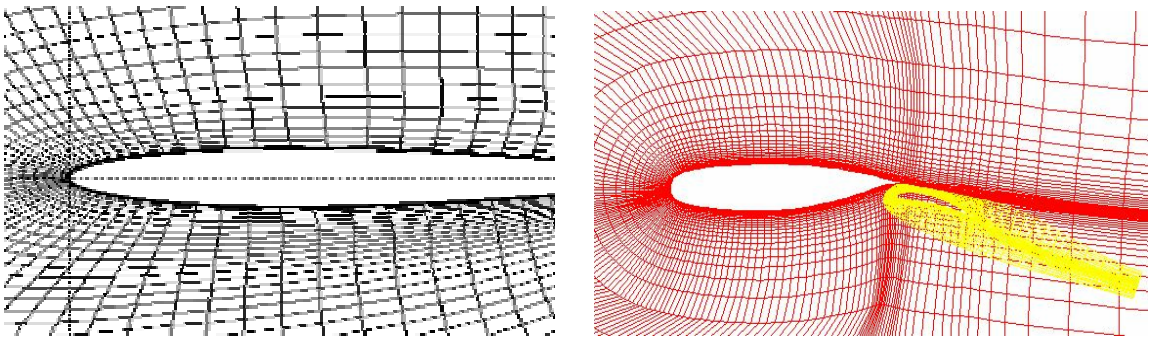

(a) (b)

Figure 7. Examples of structured grids (a) single block structured grid (b) Overset structured grid

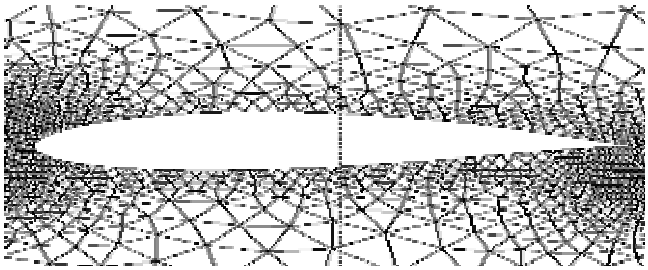

Figure 8. Example of an unstructured grid

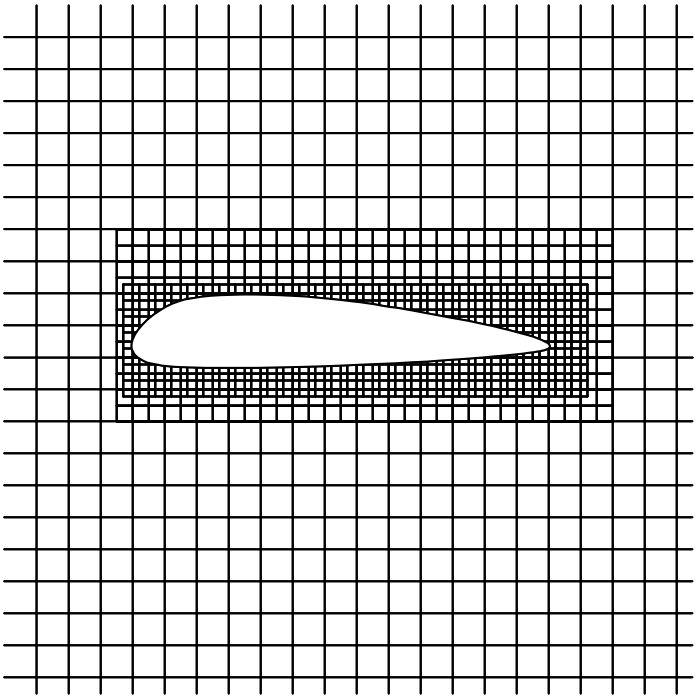

Figure 9. Example of a non-conformal Cartesian grid for flow over an airfoil with block refinement around the airfoil.

	Re	h_1^*	k	α_1	ϕ
Tuncer & Platzer [15]	10^3 -10^5	0.0125-1.0	0.5-7.85	0^o - 20^o	30^o,75^o,90^o
Isogai et al. [23]	10^5	1.0, 2.0	0.0-1.0	10^o, 20^o	30^o-150^o
Ramamurti et al. [47]	10^4, 10^3	0, 1	0-14	2,4, 15	30^o-140^o

Table 1: Parameters covered in RANS studies.

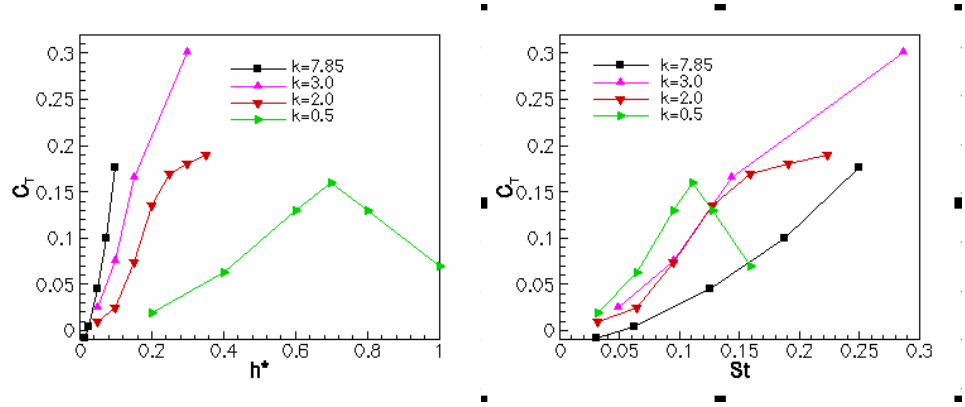

(a) (b)

Figure 10. (a) Variation of thrust with amplitude h*and frequency k for a foil undergoing plunge oscillations as computed by Tuncer & Plazer [15]. (b) Data replotted using Strouhal number (St) shows better collapse.

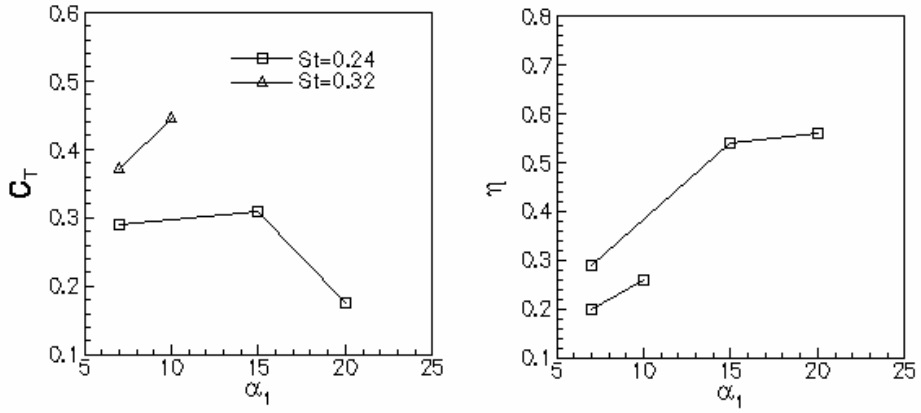

Figure 11. Effect of pitch amplitude and Strouhal number on thrust for airfoil undergoing combined pitch and heave. ($h_1^* = 0.75$, $\phi = 75^o$). Results from computations of Tuncer & Platzer [15]

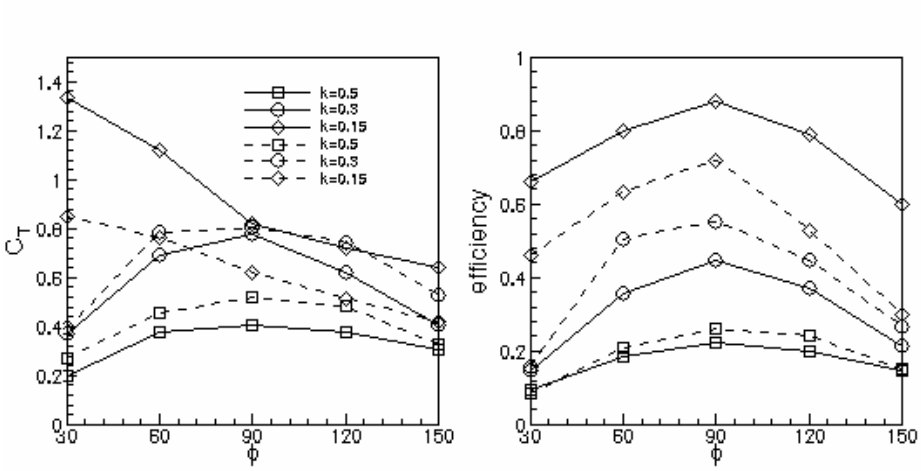

Figure 12. Effect of phase between pitch and plunge motions on thrust and efficiency. Comparison of Tuncer & Platzer [15] (solid lines) and Isogai et al.[46] (dashed lines) data.

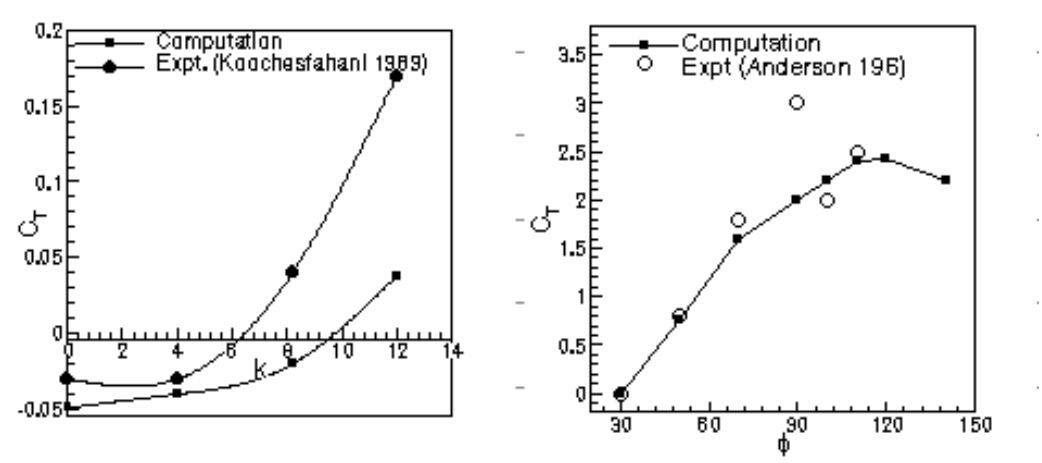

(a) (b)

Figure 13. Comparison between simulations (Ramamurti et al.) and experiments (Koochesfehani [48]) and Anderson [7]. (a) Effect of frequency parameter for pitch oscillations of 2^o at $Re=1.2x10^{4.}$.(b) effect of phasing between pitch and plunge motion for k=3.8 and $Re=1.1x10^3$.

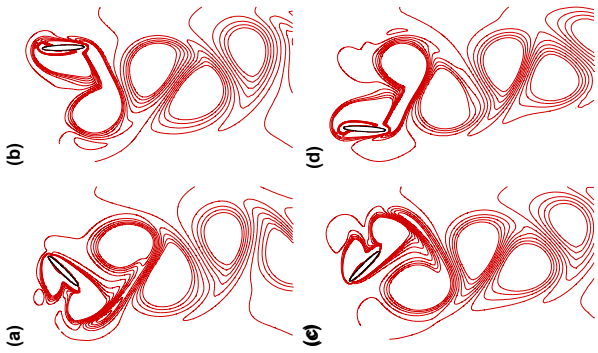

(i)

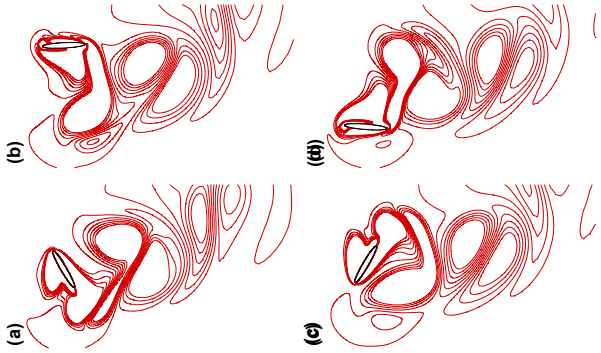

(ii)

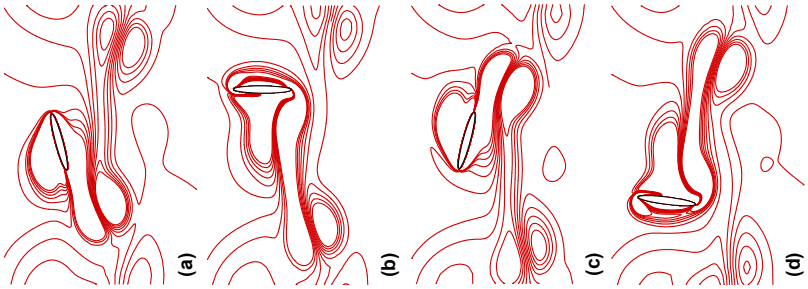

(iii)

Figure 14. Wake topologies for a flapping foil in hover computed in Ref [44]. Vortex street for $\alpha_1 = 45^o$ (ii) Vortex dipoles for $\alpha_1 = 60^o$ (iii) Pair of vortex dipoles at $\alpha_1 = 75^o$

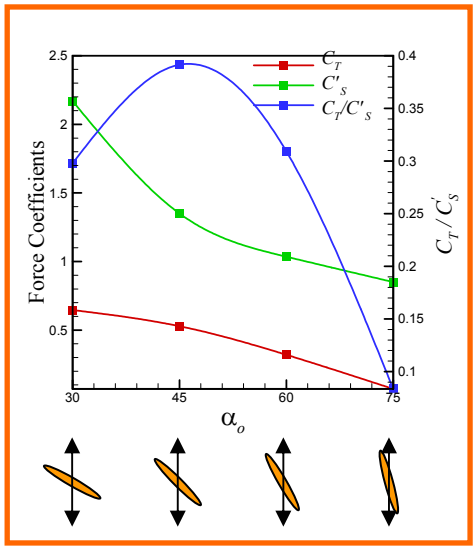

Figure 15. Variation of thrust and side force with pitch amplitude for an airfoil in hover. Optimal performance is observed for case where inverse Karman vortex street is formed.

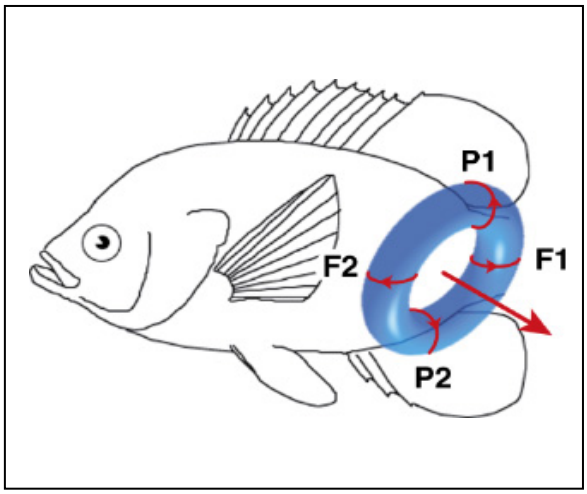

Figure 16. Schematic 3D representation of the vortex ring formed in the wake of the pectoral fin of a sunfish (Drucker and Lauder [2]).

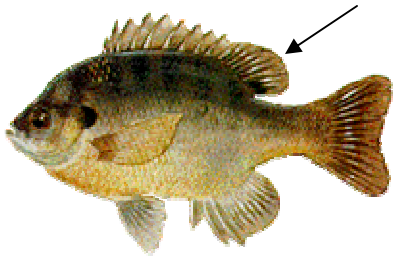

Figure 17. Bluegill sunfish with soft dorsal fin indicated

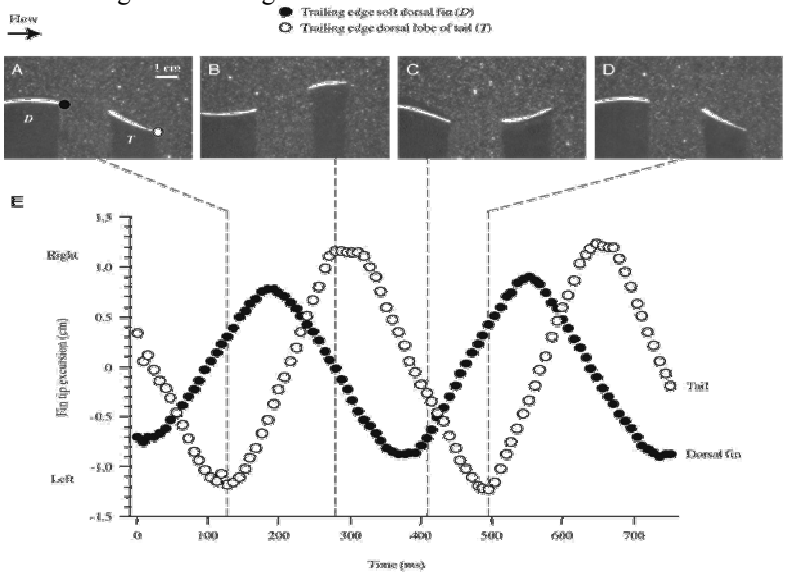

Figure 18. Motion of the trailing edges of the soft dorsal and tail fins extracted from experiments of Drucker & Lauder [2]

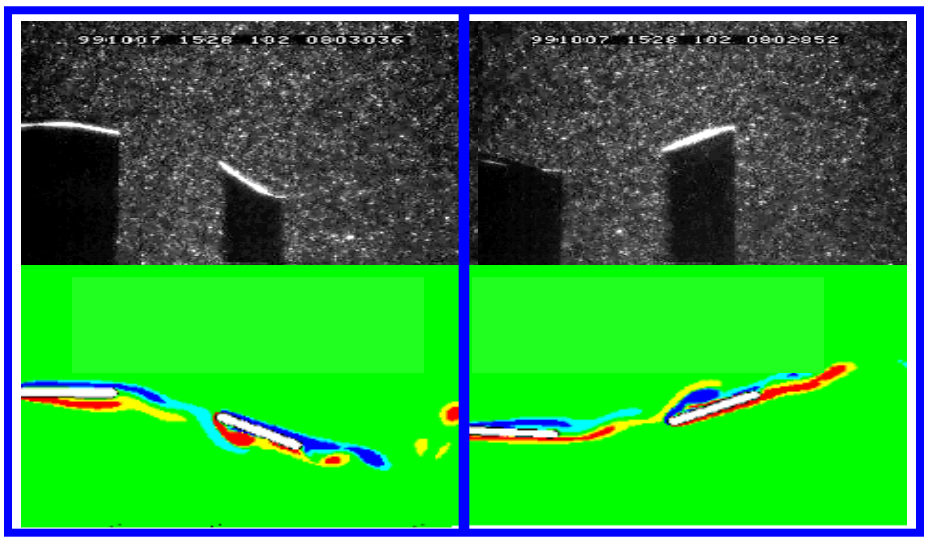

Figure 19. Qualitative comparison of experiments and computations. Lower plots shows computed spanwise vorticity contours.

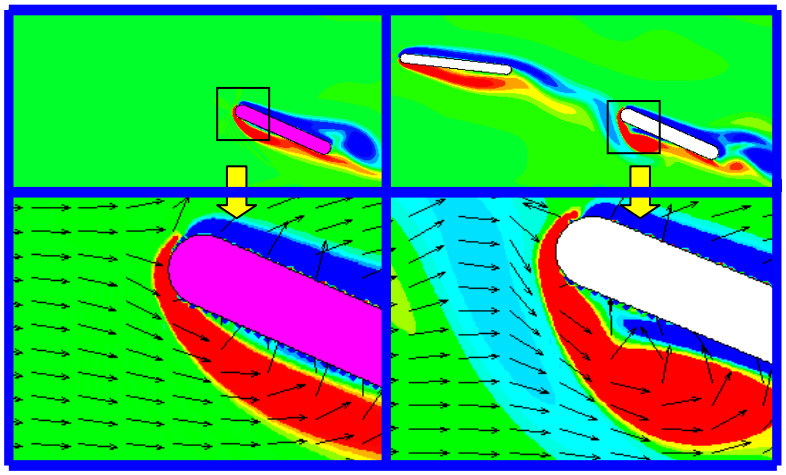

(a) (b)

Figure 20. Comparison of computed flow past tail fin (a) without and (b) with upstream dorsal fin.

Figure 21. Brooktrout with adipose fin indicated (courtesy of G. Lauder)

(a) (b)

Figure 22 (a) humpback whale flipper. (b) Hammerhead cephalofoil. Photo © Stephen M. Kajiura